VIP Hydrogen Bonding Very Important Paper

International Edition: DOI: 10.1002/anie.201505934
German Edition: DOI: 10.1002/ange.201505934

Unusual H-Bond Topology and Bifurcated H-bonds in the 2-Fluoroethanol Trimer

*Javix Thomas, Xunchen Liu, Wolfgang Jäger, and Yunjie Xu**

Abstract: *By using a combination of rotational spectroscopy and ab initio calculations, an unusual H-bond topology was revealed for the 2-fluoroethanol trimer. The trimer exhibits a strong heterochiral preference and adopts an open OH···OH H-bond topology while utilizing two types of bifurcated H-bonds involving organic fluorine. This is in stark contrast to the cyclic OH···OH H-bond topology adopted by trimers of water and other simple alcohols. The strengths of different H-bonds in the trimer were analyzed by using the quantum theory of atoms in molecules. The study showcases a remarkable example of a chirality-induced switch in H-bond topology in a simple transient chiral fluoroalcohol. It provides important insight into the H-bond topologies of small fluoroalcohol aggregates, which are proposed to play a key role in protein folding and in enantioselective reactions and separations where fluoroalcohols serve as a (co)solvent.*

Noncovalent interactions involving organic fluorine exert an enormous influence on the biological, chemical, and pharmaceutical properties of fluorinated compounds.[1] Fluoroalcohols are well known co-solvents for studying the secondary and tertiary substructures of polypeptides and proteins in aqueous solution.[2] More recently, their applications have been extended to enantioselective hydrogenations with chiral self-assembling catalysts and to enantioselective separations of a number of chiral metal–organic frameworks.[3] One important property of these fluoroalcohols is their transient chirality, which enables chirality induction, amplification, and synchronization events.[4a,b] Another interesting aspect is how well organic fluorine can serve as a hydrogen (H)-bond acceptor, a subject that is being actively researched and hotly debated.[5] While spectroscopic techniques such as NMR, FTIR, and electronic circular dichroism have greatly enriched our understanding of the roles of fluoroalcohols in the aforementioned processes, the mechanisms of these fascinating events are still not well understood. Although small clusters of fluoroalcohols have been identified as playing a key role in protein folding through the aid of molecular dynamics simulations,[6] detailed information on the H-bond topologies, especially the role of organic fluorine, is still lacking. To fully appreciate these complex events involving fluoroalcohols, a rigorous description of small fluoroalcohol clusters is essential. Suhm and co-workers have taken a bottom-up approach by studying dimers and trimers of fluoroalcohols with and without water by using low resolution jet-cooled FTIR and Raman spectroscopy.[4] By adding one solvent molecule at a time, detailed structural and energetic information about the crucial initial few steps of solvation and self-aggregation can be obtained and used as a benchmark to further improve the related theoretical modelling.

High-resolution FT microwave (MW) spectroscopy provides significant advantages in distinguishing the conformers of monomers or aggregates because their unique moments of inertia and dipole selection rules lead to well separated rotational transition frequencies.[7–9] The recent triumph of FTMW spectroscopy in detecting and providing detailed structural and energetic information about small to mid-sized water clusters highlights these advantages and demonstrates the importance of such stringent experimental tests for advancing theoretical modelling.[10] Because of the significant challenges in assigning their rotational spectra, very few FTMW studies of trimers and higher clusters of organic molecules have been reported so far. Examples are trimers and tetramers of difluoromethane held together by weak H-bonds[11] and the phenol trimer.[12b] Herein, we report a detailed FTMW spectroscopic and ab initio study of the trimer of the transiently chiral 2-fluoroethanol (FE). Our study reveals an unusual H-bond topology for the FE trimer and significant roles for OH···FC and bifurcated H-bonds in stabilizing the particular binding arrangement.

In contrast to water and ethanol, FE has both hydrophobic and hydrophilic domains and an F atom that can act as an H-bond acceptor. While ethanol exhibits subtle *gauche–trans* isomerism, both FE and trifluoroethanol (TFE) exist in one dominant *gauche* form.[4a,13] Previous molecular self-recognition studies on the dimer of FE[4c,14] show only a slight preference for the heterochiral species, while the TFE dimer[4a,15] exhibits a strong homochiral preference. In the liquid state, on the other hand, the *trans*/*gauche* ratio increases to 40:60 for TFE, whereas the *trans* form of FE is only slightly populated even at a much elevated temperature of 156 °C.[16] It is thus of great interest to evaluate the effects of monomeric conformational distribution, the associated transient chirality, and the H-bond interactions with fluorine in small clusters of FE and eventually to make a connection to the microstructures in the FE liquid.

In terms of the detailed H-bond topology of trimers, water and the small alcohols methanol and ethanol have been shown to favour a cyclic H-bonded ring structure in which

[*] Dr. J. Thomas, Prof. Dr. W. Jäger, Prof. Dr. Y. Xu
Department of Chemistry, University of Alberta
Edmonton, Alberta, T6G 2G2 (Canada)
E-mail: yunjie.xu@ualberta.ca
Dr. X. Liu
School of Mechanical Engineering, Shanghai Jiao Tong University
No.800 Dong Chuan Road, Shanghai, 200240 (P.R. China)

Supporting information for this article is available on the WWW under http://dx.doi.org/10.1002/anie.201505934.

each molecule serves simultaneously as an H-bond donor and acceptor, utilizing the classical OH···OH H-bonds and emphasizing cooperativity.[17–19] Both TFE[4a] and phenol[12] were reported to have a cyclic OH···OH H-bonded ring for their most stable ternary clusters, even though phenol includes a bulky aromatic unit. Similarly, methyl lactate, a derivative of methanol, exhibits an analogous cyclic H-bonded ring and strongly favours the homochiral ternary combination.[4b,20] We note that no previous structural identification was reported for the FE trimer, although some IR bands observed in a jet expansion were tentatively identified as being due to FE clusters beyond the dimer.[4c]

To aid with the spectral search, extensive ab initio calculations were carried out to explore the conformational landscape of the FE trimer. FE is a transiently chiral species with two structurally relevant dihedral angles, τ(FCCO) and τ(CCOH), which can take on $g+$ (+60°), $g-$ (−60°), and t (0°) conformations. The monomer therefore has nine possible conformations, including four enantiomeric pairs, classified into five groups: $G-g+/G+g-$, $G-t/G+t$, Tt, $Tg-/Tg+$, and $G-g-/G+g+$, in order of decreasing stability. The capital and small letters stand for τ(FCCO) and τ(CCOH), respectively. Based on the related trimer structures, similar cyclic OH···OH H-bonded ring structures were explored for the FE trimer with subtly different orientations of the hydroxy and aliphatic/fluorinated parts. One particularly aesthetic structure is conformer **II** (Figure 1), an oblate symmetric top in which two intermolecular H-bonded rings coexist to give the usual cyclic OH···OH and a CH···FCH H-bonded ring. This homochiral conformer is the most stable cyclic ring structure identified and has a large *c*-type dipole moment component. One therefore expects an easily recognizable symmetric top spectral pattern. Despite intensive efforts since 2008, no spectrum could be assigned based on this or any other related cyclic H-bonded ring structures.[21]

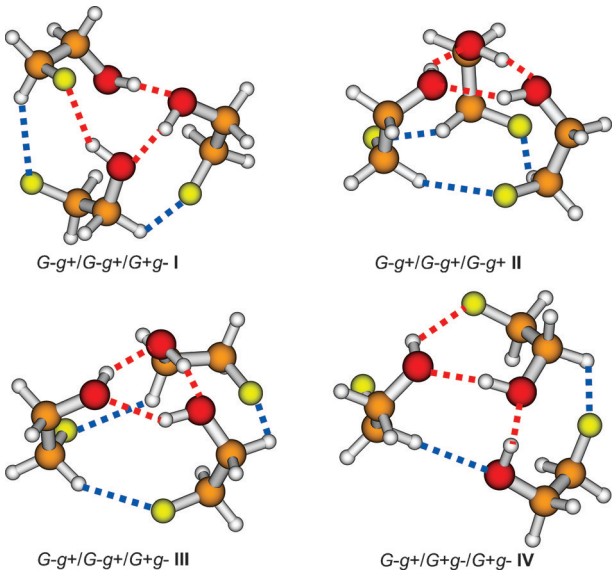

Figure 1. Geometries of the four most stable conformers of the FE trimer. C orange, O red, F yellow. The OH···OH and OH···FC H-bonds are shown in red and CH···FC/CH···OH H-bonds in blue.

The unsuccessful trials indicated that the FE trimer perhaps takes on a drastically different binding topology.

Although only the $G-g+/G+g-$ enantiomeric pair was detected as the monomer and as the building block in the FE dimer experimentally (the next monomeric enantiomeric pair is more than 7 kJ mol^{-1} less stable),[4c,14] we considered all possible ternary combinations of the monomeric subunits from the above five groups, giving 125 starting geometries. Furthermore, we recognized that chirality plays an important role in the conformational stability of the ternary system and more subtle conformal changes were thus explored by switching the chirality of particular subunits in a FE trimer. The structures of 28 low-energy conformers were re-optimized at the MP2/6-311++G(2d,p) level and their true minimum natures were confirmed by harmonic frequency calculations. The geometries of the four most stable conformers are shown in Figure 1 and their calculated relative energies and spectroscopic constants are given in Table 1, while the corresponding information for the other less stable conformers is provided in Figure S1 and Table S1 in the Supporting Information.

The conformers of the FE trimer are named for their monomeric constituents and their relative stability ranking is indicated by Roman numerals, with **I** being the most stable. For simplicity, we will use Roman numerals to denote particular conformers in the remainder of the paper. Not surprisingly, all four of the most stable conformers are made of the $G+g-/G-g+$ monomeric subunits. What is surprising is that the predicted most stable trimer (**I**) is heterochiral and does not possess a cyclic OH···OH H-bonded ring. The homochiral oblate top (**II**), which has the usual OH···OH cyclic ring, is approximately 3.3 kJ mol^{-1} less stable, or 0.9 kJ mol^{-1} after *BSSE* correction, than **I**. As can be seen from Table 1, **I** and **II** are expected to have vastly different rotational transition frequencies, obeying different selection rules. In fact, all four conformers can be easily identified by their rotational spectra.

Preliminary searches for the FE trimer were done by using a chirped pulse (CP) and a cavity-based FTMW spectrome-

Table 1: Relative energies and spectroscopic constants of the four most stable conformers of the FE trimer at the MP2/6-311++G(2d,p) level of theory.

Parameter[a]	I	II	III	IV
ΔD_e	0.00	4.15	5.23	5.63
ΔD_e^{BSSE}	0.00	1.77	2.79	3.22
ΔD_0	0.00	3.32	4.55	4.74
ΔD_0^{BSSE}	0.00	0.93	2.11	2.32
A	844	677	798	895
B	610	677	582	481
C	455	465	438	388
$\lvert\mu_a\rvert$	1.33	0.00	0.03	1.84
$\lvert\mu_b\rvert$	0.74	0.00	0.00	1.50
$\lvert\mu_c\rvert$	1.12	2.07	2.21	0.41

[a] ΔD_e, ΔD_e^{BSSE}, ΔD_0, ΔD_0^{BSSE} are the raw, basis set superposition error (*BSSE*)-corrected,[26] zero-point energy (*ZPE*)-corrected, and both *ZPE*- and *BSSE*-corrected relative dissociation energies in kJ mol^{-1}, respectively. *A*, *B*, and *C* are rotational constants in MHz, and $\lvert\mu_{a,b,c}\rvert$ is the magnitude of the electric dipole moment components in Debye.

Table 2: Experimental spectroscopic parameters of the FE trimer.

Parameter	I
A [MHz]	828.79997(18)
B [MHz]	596.39423(11)
C [MHz]	441.971596(94)
D_J [kHz]	0.12440(65)
D_{JK} [kHz]	−0.0674(51)
D_K [kHz]	0.4588(54)
d_1 [kHz]	−0.03558(37)
d_2 [kHz]	−0.00501(26)
N[a]	60
σ [kHz][b]	1.7

[a] The number of transitions included in the fit. [b] The standard deviation of the fit. Standard errors are in parentheses and are expressed in units of the least significant digit.

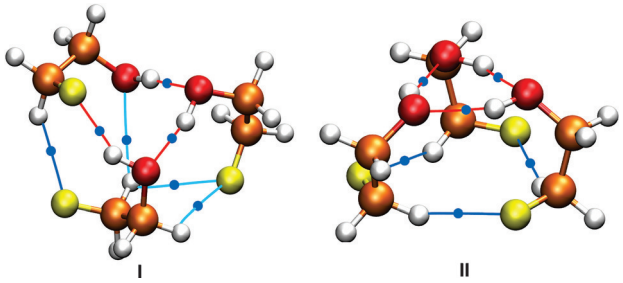

Figure 2. QTAIM analyses of the ternary FE conformers **I** and **II**. C orange, O red, F yellow. The BCPs are indicated with blue dots, except for those of the covalent bonds which are omitted for clarity. The bond paths for the OH···H and OH···FC H-bonds are shown in red, those for the CF···HC H-bonds in dark blue, and those for the bifurcated H-bonds in cyan.

ter[22,23] in the 7.7–11.7 and 3.7–7.7 GHz regions, respectively. Strong transitions resulting from the FE monomer[13] and dimer[14] could be eliminated, thereby greatly facilitating the spectral assignment of the FE trimer. A total of 60 observed transitions of *a*-, *b*- and *c*-types were assigned and fitted by using Watson's *S*-reduction[24] Hamiltonian in its I^r representation with the Pgopher program.[25] The experimental spectroscopic constants are summarized in Table 2, while the fitted transition frequencies are summarized in Table S2 in the Supporting Information. The experimental rotational constants and the relative *a*-, *b*- and *c*-type transition intensities are consistent only with **I**, with the maximum deviation of the experimental constants from the theoretical ones being approximately 2.9%. The signs of the distortion constants were also reproduced by a harmonic force field calculation of **I**.

Considerable efforts were spent to identify spectra of **II**–**IV** but without success. We note that the remaining unassigned transitions are considerably weaker than those assigned to **I**. Therefore, the current experimental data show that **I** is by far the preferred binding topology utilized by the FE trimer. This experimental observation suggests that the relative energy difference between **I** and the rest (**II**, **III**, and **IV**) is likely to be larger than 1 kJ mol^{-1} and is probably close to 4 kJ mol^{-1}, as indicated by the ΔD_0 values. As noted in a previous FE dimer study[14] and by others,[27] the counterpoise correction[26] tends to overcorrect with relatively small basis sets such as the one used here.

It is not immediately obvious why **I** is the preferred binding topology over **II** when examining the optimized geometries of **I** and **II** (Figure 1). Since weak H-bonds are often found alongside strong ones, they are hard to identify, even though their significant contribution to self-assembly, crystallisation, and other molecular recognition processes is being increasingly recognized.[28] To appreciate the stability of **I**, we applied Bader's quantum theory of atoms in molecules (QTAIM),[29] a powerful method for characterizing H-bonds.[30,31] We utilized the Multiwfn[32] program and performed QTAIM analyses to identify bond critical points (BCPs) and bond paths of potential H-bonds. The results for **I** and **II** are illustrated in Figure 2. While the H-bonds identified in Figure 1 are all confirmed for **I** and **II** in the QTAIM analyses, two different types of bifurcated H-bonds[33] were additionally identified in **I** and none in **II**. In the first type of bifurcated H-bonds, (C)H acts as an H-donor to both O and F atoms, while in the second type, F acts as a bifurcated acceptor for two adjacent (C)H atoms. The unexpected stability of **I** may be a result of these bifurcated H-bonds (see below).

Bifurcated H-bonds are commonly identified in the crystal structures of biomolecules such as amino acids, nucleobases, and sugars.[34] The strength of a bifurcated H-bond, for example, between a thiol (or hydroxy) H^+ and C=O was shown recently to be between 50 to 60% of that of canonical H-bonds.[35] The H-bond energy E_{HB} can be estimated by using $E_{HB} = 0.5\,a_0^3\,V(r)$, where $V(r)$ is the electron potential density at the related BCP and a_0 is the Bohr radius.[36] The energy values for the H-bonds identified in **I** and **II** are given in Table S3 in the Supporting Information. The sum of all H-bond energies is 143.6 kJ mol^{-1} for **I**, which is much larger than the 110.8 kJ mol^{-1} calculated for **II**. While we acknowledge that E_{HB} values based on $V(r)$ are known to be overestimated, the relative magnitudes of the E_{HB} values nevertheless show a clear preference for **I** over **II**, consistent with the experimental data. While the CH···FC bond energies, at approximately 8 to 9 kJ mol^{-1}, are similar in **I** and **II,** the E_{HB} values range from 5 to 8 kJ mol^{-1} for the three bifurcated H-bonds identified in **I**. Furthermore, opening up the strained OH···OH cyclic H-bonds in **II** allows **I** to have two stronger OH···OH H-bonds and an additional OH···FC H-bond. A detailed analysis shows that the strength of the OH···OH bonds in **I** comes from the fact that these bonds adopt a much closer to linear arrangement (171° and 164°) compared to those in **II** (146°). All of these factors result in a strong preference for **I** over **II**. It is worth emphasizing that in comparison to the homochiral trimer **II**, which adopts the usual cyclic OH···OH H-bonded ring topology, the experimentally identified FE trimer **I** is heterochiral and takes on a very different H-bond topology, with two OH···OH bonds and one OH···FC H-bond, supplemented with three bifurcated H-bonds. This is a striking case of a chirality-induced switch in H-bond topology. Related chirality-dependent switching in H-bond topology has been reported for tetrameric methyl lactate clusters and 1-indanol clusters.[37]

In summary, an unusual H-bond topology in the FE trimer was revealed by using FTMW spectroscopy and ab initio calculations. In contrast to related small hydroxy-group-containing molecules, such as water, methanol, ethanol, TFE, phenol, and methyl lactate, all of which adopt a cyclic OH···OH H-bonded ring in their most stable trimer, the FE trimer shows a strong heterochiral preference and adopts a compact binding topology that utilizes OH···OH, OH···FC and two types of bifurcated H-bonds. The QTAIM analyses offer insights into the preference for heterochiral **I** over homochiral **II**, which assumes the usual cyclic H-bonded ring. This study showcases a remarkable example of a chirality-induced switch in H-bond topology in a simple fluoroalcohol trimer and highlights the importance of bifurcated H-bonds in even a relatively small cluster. It provides new insight into the initial few steps of the self-aggregation of a widely used fluoroalcohol.

Experimental Section

Spectral measurements were done using a CP- and a cavity-based FTMW spectrometer, the details of which were described before.[22,23] For the final measurements with the cavity-based instrument, the frequency uncertainty is ca. 2 kHz and the full line width at half maximum is ca. 10 kHz. An FE sample obtained from Sigma Aldrich (97 % purity) was used without further purification. A sample mixture of 0.1 % FE in 2–4 bar of helium or neon was used for the CP and the cavity measurements, respectively. We used the Gaussian 09 program package[38] for all geometry optimization and harmonic-frequency calculations. All final results were obtained at the second order Møller-Plesset perturbation theory (MP2)[39] level with the 6-311++G(2d,p) basis set.[40] The cartesian coordinates of **I** and **II** are listed in Table S4.

Acknowledgements

This research was funded by the University of Alberta and the Natural Sciences and Engineering Research Council (NSERC) of Canada. We thank Elijah G. Schnitzler for discussions about AIM analyses. We also gratefully acknowledge access to the computing facilities of the Shared Hierarchical Academic Research Computing Network (SHARCNET: www.sharcnet.ca), the Western Canada Research Grid (Westgrid), and Compute/Calcul Canada. W.J. and Y.X. are holders of Tier I Canada Research Chairs.

Keywords: bifurcated H-bonds · chirality · fluoroalcohols · H-bond topology · rotational spectroscopy

How to cite: *Angew. Chem. Int. Ed.* **2015**, *54*, 11711–11715
Angew. Chem. **2015**, *127*, 11877–11881

[1] a) K. Müller, C. Faeh, F. Diederich, *Science* **2007**, *317*, 1881–1886; b) R. Berger, G. Resnati, P. Metrangolo, E. Weber, J. Hulliger, *Chem. Soc. Rev.* **2011**, *40*, 3496–3508.

[2] a) M. Buck, *Q. Rev. Biophys.* **1998**, *31*, 297–355; b) M. Fioroni, M. D. Diaz, K. Burger, S. Berger, *J. Am. Chem. Soc.* **2002**, *124*, 7737–7744.

[3] a) N. V. Dubrovina, I. A. Shuklov, M.-N. Birkholz, D. Michalik, R. Paciello, A. Börner, *Adv. Synth. Catal.* **2007**, *349*, 2183–2187; b) H. C. Hoffmann, S. Paasch, P. Müller, I. Senkovska, M. Padmanaban, F. Glorius, S. Kaskel, E. Brunner, *Chem. Commun.* **2012**, *48*, 10484–10486.

[4] a) T. Scharge, C. Cézard, P. Zielke, A. Schütz, C. Emmeluth, M. A. Suhm, *Phys. Chem. Chem. Phys.* **2007**, *9*, 4472–4490; b) T. Scharge, T. N. Wassermann, M. A. Suhm, *Z. Phys. Chem.* **2008**, *222*, 1407–1452; c) T. Scharge, C. Emmeluth, T. Haber, M. A. Suhm, *J. Mol. Struct.* **2006**, *786*, 86–95; d) M. Heger, T. Scharge, M. A. Suhm, *Phys. Chem. Chem. Phys.* **2013**, *15*, 16065–16073.

[5] a) J. D. Dunitz, R. Taylor, *Chem. Eur. J.* **1997**, *3*, 89–98; b) H.-J. Schneider, *Chem. Sci.* **2012**, *3*, 1381–1394; c) G. T. Giuffredi, V. Gouverneur, B. Bernet, *Angew. Chem. Int. Ed.* **2013**, *52*, 10524–10528; *Angew. Chem.* **2013**, *125*, 10718–10722.

[6] a) D.-P. Hong, M. Hoshino, R. Kuboi, Y. Goto, *J. Am. Chem. Soc.* **1999**, *121*, 8427–8433; b) D. Roccatano, G. Colombo, M. Fioroni, A. E. Mark, *Proc. Natl. Acad. Sci. USA* **2002**, *99*, 12179–12184; c) R. M. Culik, R. M. Abaskharon, I. M. Pazos, F. Gai, *J. Phys. Chem. B* **2014**, *118*, 11455–11461.

[7] Y. Xu, W. Jäger in *Handbook of High-resolution Spectroscopy* (Eds.: M. Quack, F. Merkt), Wiley, Chichester, **2011**, pp. 917–937.

[8] a) L. Evangelisti, G. Feng, P. Écija, E. J. Cocinero, F. Castaño, W. Caminati, *Angew. Chem. Int. Ed.* **2011**, *50*, 7807–7810; *Angew. Chem.* **2011**, *123*, 7953–7956; b) I. Peña, E. J. Cocinero, C. Cabezas, A. Lesarri, S. Mata, P. Écija, A. M. Daly, Á. Cimas, C. Bermúdez, F. J. Basterretxea, S. Blanco, J. A. Fernández, J. C. López, F. Castaño, J. L. Alonso, *Angew. Chem. Int. Ed.* **2013**, *52*, 11840–11845; *Angew. Chem.* **2013**, *125*, 12056–12061.

[9] a) J. Thomas, W. Jäger, Y. Xu, *Angew. Chem. Int. Ed.* **2014**, *53*, 7277–7280; *Angew. Chem.* **2014**, *126*, 7405–7408; b) J. Thomas, O. Sukhrukov, W. Jäger, Y. Xu, *Angew. Chem. Int. Ed.* **2014**, *53*, 1156–1159; *Angew. Chem.* **2014**, *126*, 1175–1178.

[10] a) C. Pérez, M. T. Muckle, D. P. Zaleski, N. A. Seifert, B. Temelso, G. C. Shields, Z. Kisiel, B. H. Pate, *Science* **2012**, *336*, 897–901; b) C. Pérez, S. Lobsiger, N. A. Seifert, D. P. Zaleski, B. Temelso, G. C. Shields, Z. Kisiel, B. H. Pate, *Chem. Phys. Lett.* **2013**, *571*, 1–15.

[11] a) S. Blanco, S. Melandri, P. Ottaviani, W. Caminati, *J. Am. Chem. Soc.* **2007**, *129*, 2700–2703; b) G. Feng, L. Evangelisti, I. Cacelli, L. Carbonaro, G. Prampolini, W. Caminati, *Chem. Commun.* **2014**, *50*, 171–173.

[12] a) T. Ebata, T. Watanabe, N. Mikami, *J. Phys. Chem.* **1995**, *99*, 5761–5764; b) N. A. Seifert, A. L. Steber, J. L. Neill, C. Perez, D. P. Zaleski, B. H. Pate, A. Lesarri, *Phys. Chem. Chem. Phys.* **2013**, *15*, 11468–11477.

[13] K. S. Buckton, R. G. Azrak, *J. Chem. Phys.* **1970**, *52*, 5652–5655.

[14] X. Liu,, N. Borho, Y. Xu, *Chem. Eur. J.* **2009**, *15*, 270–277.

[15] J. Thomas, Y. Xu, *J. Phys. Chem. Lett.* **2014**, *5*, 1850–1855.

[16] a) K. Hagen, K. Hedberg, *J. Am. Chem. Soc.* **1973**, *95*, 8263–8266; b) I. Bakó, T. Radnai, M. Claire, B. Funel, *J. Chem. Phys.* **2004**, *121*, 12472–12480.

[17] a) N. Pugliano, R. A. Saykally, *Science* **1992**, *257*, 1937–1940; b) F. N. Keutsch, J. D. Cruzan, R. J. Saykally, *Chem. Rev.* **2003**, *103*, 2533–2577.

[18] R. A. Provencal, J. B. Paul, K. Roth, C. Chapo, R. N. Casaes, R. J. Saykally, G. S. Tschumper, H. F. Schaefer III, *J. Chem. Phys.* **1999**, *110*, 4258–4267.

[19] M. Ehbrecht, F. Huisken, *J. Phys. Chem. A* **1997**, *101*, 7768–7777.

[20] N. Borho, M. A. Suhm, *Org. Biomol. Chem.* **2003**, *1*, 4351–4358.

[21] X. Liu, N. Borho, Y. Xu, 2008-RH-02: http://hdl.handle.net/1811/33561.

[22] Y. Xu, W. Jäger, *J. Chem. Phys.* **1997**, *106*, 7968–7980.

[23] a) S. Dempster, O. Sukhrukov, Q. Y. Lei, W. Jäger, *J. Chem. Phys.* **2012**, *137*, 174303; b) J. Thomas, J. Yiu, J. Rebling, W. Jäger, Y. Xu, *J. Phys. Chem. A* **2013**, *117*, 13249–13254.

[24] J. K. G. Watson in *Vibrational Spectra and Structure*, *Vol. 6* (Ed.: J. R. Durig), Elsevier, New York, **1977**, pp. 1–89.

[25] Pgopher, a Program for Simulating Rotational structure, C. M. Western, University of Bristol, http://Pgopher.chm.bris.ac.uk.
[26] S. F. Boys, F. Bernardi, *Mol. Phys.* **1970**, *19*, 553 – 566.
[27] M. Masamura, *Theo. Chem. Acc.* **2001**, *106*, 301 – 313.
[28] K. E. Riley, P. Hobza, *WIREs Comput. Mol. Sci.* **2011**, *1*, 3 – 17.
[29] a) R. F. W. Bader, *Atoms in Molecules: A Quantum Theory*, Oxford University Press, New York, **1990**; b) R. F. W. Bader, *Chem. Rev.* **1991**, *91*, 893 – 928; c) P Popelier, *Atoms in Molecules: An Introduction*, Prentice Hall, Harlow, **2000**.
[30] a) P. L. A. Popelier, R. F. W. Bader, *Chem. Phys. Lett.* **1992**, *189*, 542 – 548; b) M. Petković, M. Etinski, *RSC Adv.* **2014**, *4*, 38517 – 38526.
[31] a) J. R. Cheeseman, M. T. Carroll, R. F. W. Bader, *Chem. Phys. Lett.* **1988**, *143*, 450 – 458; b) O. O. Brovarets', R. O. Zhurakivsky, D. M. Hovorun, *J. Comput. Chem.* **2014**, *35*, 451 – 466.
[32] T. Lu, F. Chen, *J. Comput. Chem.* **2012**, *33*, 580 – 592.
[33] I. Rozas, I. Alkorta, J. Elguero, *J. Phys. Chem. A* **1998**, *102*, 9925 – 9932.
[34] a) G. A. Jeffrey, J. Mitra, *J. Am. Chem. Soc.* **1984**, *106*, 5546 – 5553; b) J. A. Ballesteros, X. Deupi, M. Olivella, E. E. Haaksma, L. Pardo, *Biophys. J.* **2000**, *79*, 2754 – 2760.
[35] E. S. Feldblum, I. T. Arkin, *Proc. Natl. Acad. Sci. USA* **2014**, *111*, 4085 – 4090.
[36] a) E. Espinosa, E. Molins, C. Lecomte, *Chem. Phys. Lett.* **1998**, *285*, 170 – 173; b) I. Mata, I. Alkorta, E. Espinosa, E. Molins, *Chem. Phys. Lett.* **2011**, *507*, 185 – 189.
[37] a) T. B. Adler, N. Borho, M. Reiher, M. A. Suhm, *Angew. Chem. Int. Ed.* **2006**, *45*, 3440 – 3445; *Angew. Chem.* **2006**, *118*, 3518 – 3523; J. Altnöder, A. Bouchet, J. J. Lee, K. E. Otto, M. A. Suhm, A. Zehnacker-Rentien, *Phys. Chem. Chem. Phys.* **2013**, *15*, 10167 – 10180.
[38] Gaussian 09 (Revision C.01): M. J. Frisch, et al. See the Supporting Information for the full reference.
[39] C. Møller, M. S. Plesset, *Phys. Rev.* **1934**, *46*, 618 – 622.
[40] a) J. S. Binkley, J. A. Pople, *Int. J. Quantum Chem.* **1975**, *9*, 229 – 236; b) R. Krishnan, J. S. Binkley, R. Seeger, J. A. Pople, *J. Chem. Phys.* **1980**, *72*, 650 – 654.

Received: June 28, 2015
Published online: August 14, 2015

